EARTH/MOON IMPACT RATE COMPARISON: POSSIBLE CONSTRAINTS FOR LUNAR SECONDARY/PRIMARY CRATERING PROPORTION.

B.A Ivanov, Institute for Dynamics of Geospheres, RAS, 119334, Moscow, Russia, baivanov@idg.chph.ras.ru.

Introduction: Published data for global impact rate of bolides are compared with the cratering rate on the moon in the past 100 Ma (assumed to be constant). The comparison shows, that in the limits of used models accuracy, the current meteoroid flux in the Earth-moon system is approximately the same as in the last 100 Ma, provided most of the small (*D*<200 m) craters counted on the young (<100 Ma) lunar surface are primary, not secondary craters.

Global impact rate of bolides: The satellite records of bolide detonation in Earth's atmosphere [1, 2] present the frequency of light (flash) bursts during the atmospheric entry of small (less than 10 m in diameter) meteoroids. Without additional information, the mass, velocity, and composition of these meteoroids are not known from the flash records only. However, this is a unique database for the present day bombardment flux in the Earth-moon system. The total kinetic energy of meteoroids is estimated theoretically and by comparison with other kinds of registration [1,2]. In average, the optical detonation energy, measured by satellite sensors, is close to 10% of the pre-entry kinetic energy of a meteoroid, varying from 3% to 20% for most of the events calibrated in [2].

Small craters on the moon: The pioneering paper by Shoemaker et al. [3] has used crater counts for the Apollo 11 and 12 landing sites, where small craters with D>100 m (below the equilibrium line) have the cumulative SFD $N(>D) \sim D^{-n}$, where $n = 2.9 \pm 0.03$. Neukum uses the Shoemaker's $N(>D) \sim D^{-2.9}$ as an upper branch for his polynomial production function, NPF. Smaller lunar craters below the equilibrium level have been measured near the Apollo 14 and 16 landing sites for North Ray (J. Boyce), Cone (A. Watkins) and South Ray (J. Moore) craters – see [4]. These counts have been approximated with the cumulative relation $N(>D) \sim D^{-2.8}$.[4]. With the available data accuracy the population index of n=2.9 is equally plausible.

Fig. 1a shows the SFD fit to small crater data. The extrapolated intercept to $D = 1$ km results in a crater retention age estimate provided that the cratering rate is constant and N(>1 km)=8.38 10^{-4} km^{-2} Ga^{-1} [5]. All craters used here have been dated by the cosmic ray exposure (CRE) time of the last overturning of ejected boulders [6, 7], which is compared with the crater retention age in Fig. 1b. The data show a good (factor of 2 in the worst case) agreement of two techniques. This is not amazing, as CRE data have been used originally to calibrate the crater chronology. Craters of 10 m in diameter approach the equilibrium areal density at surfaces older than ~30 Ma. Hence the dating of younger surfaces with craters 10 m in diameter and smaller is impossible.

Bolide/crater impact rate comparison: To estimate the cratering rate on the moon from meteoroids, observed as bolides in [2] we assume average impact velocities on Earth and on the moon and the gravity enhancement of planetary cross-sections, related to these velocities, with the estimates having been corrected for observational biases [8]: impact velocity of 20.9 km s^{-1} on Earth, 19.2 km s^{-1} on the moon, and the Earth/moon ratio of impact flux of 1.38. Assuming oblique impacts at an average angle of 45^{o}, and an average impact velocity, given above, the kinetic energy of terrestrial bolides is recalculated to the areal crater density (*N/S*) versus rim crater diameter, *D*, for a lunar reference surface age of 1 Ma.

For lunar craters below 100 m, the dry sand looks like a reasonable proxy. Small cohesion may result in a transition to strength craters below *D*~15 m – estimates based on cratering in alluvium [9], assuming lunar regolith cohesion of ~3 kPa at least in the upper 1 m. For rim crest crater diameter published data [10, 11] give: $R_{rim} (\rho/m)^{1/3} = 1.0 (3.22\, g\, a\, (v_{imp} \sin \alpha)^{-2})^{-0.17}$, where ρ is the target density, g is gravity acceleration, m and a are projectile mass and radius, and v_{imp} and α are impact velocity and impact angle, measured from the horizon.

Bolide rate [2] recalculated to the lunar cratering rate well fit the lunar cratering rate and its dependence on the crater size (Fig. 2). The comparison of 0.1-1 kton bolide impact rate, recalculated to the moon, with the youngest lunar data available illustrates that the present-day impact flux is approximately equal to the average lunar cratering rate for the last 100 Ma.

Conclusion: The scaling law for dry sand gives smallest predictions of lunar crater sizes for a given projectile diameter (due to a low value of the velocity exponent). The soft rock (non-porous) scaling used here for megaregolith, gives larger craters even in a strength regime. This makes the bolide cratering flux *larger* than is needed to keep the observed lunar cratering rate for primary craters only. For the nominal model the lunar cratering rate corresponds to the meteoroid flux to the Earth-moon system providing that the considerable number of *counted* lunar craters are primary ones.

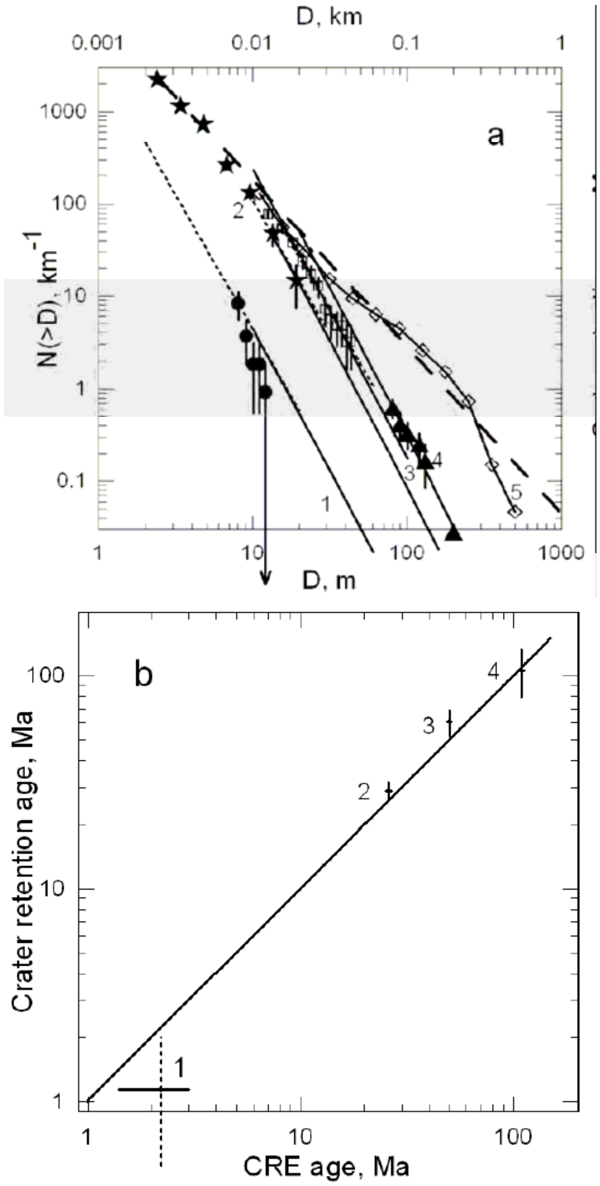

Fig. 1. (a) Cumulative crater counts for craters with D<100 m for four craters, dated with cosmic ray exposure in returned samples. 1 – South Ray crater; 2 – Cone crater, 3 – North Ray crater [4]; 4 – Tycho crater [12]. For comparison the composite crater count on an "average" lunar mare is shown (Hartmann et al., 1981), illustrated the equilibrium ("saturation") population of small craters. Dashed line presents the equilibrium as $N(>D) = 0.047\ D^{-1.83}$ [13] which well fit to small craters counted around Cone crater (2). (b) – the comparison of crater retention ages computed with Neukum's lunar geochronology [5] for D≥10 m and assuming $N(>D) \sim D^{-2.9}$ for smaller craters. 1 to 4 are for the same craters as in (a). Cosmic ray exposure (CRE) ages are from [6,7] except South Ray crater where all data from Table III in [6] are used to estimate the standard deviation. The black line shows equal crater retention and CRE ages.

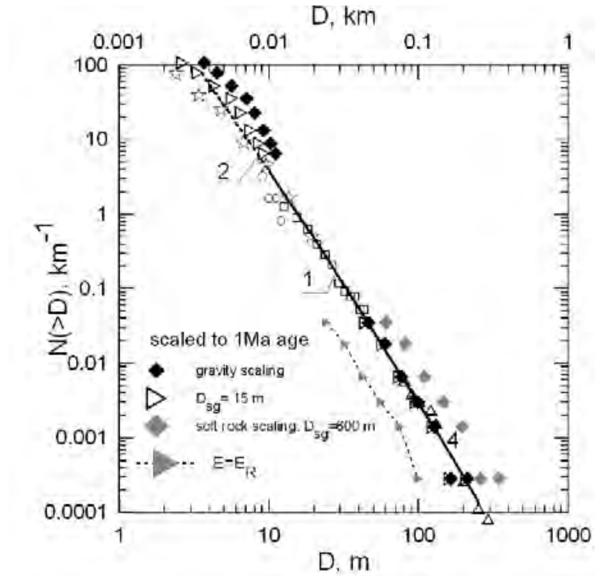

Fig. 2. Data for small lunar craters on dated surfaces, shown in Fig. 1a, scaled to the 1 Ma accumulation age (open symbols correspond to the same filled symbols in Fig. 1a). Error bars are omitted for clarity Curve 1 is the Neukum's polynomial curve, valid for D≤10 m. Dashed line 2 is the $N \sim D^{-2.9}$ exponential extrapolation of data. Triangles and diamonds are for terrestrial bolide and fireball impacts, recalculated to the accumulated number of primary lunar impact craters for 1 Ma of exposition. Black diamonds are for the nominal kinetic energy estimates [2] and dry sand (regolith proxy) cratering scaling [10]. Open rightward triangle – the same scaling with an assumed strength-gravity transition at D=15 m. Gray diamonds are for wet sand (megaregolith proxy) with an assumed strength gravity transition at D=600 m. "$E=E_R$" is for the extreme case of 100% efficiency of light flash, produced by bolides (registered light flash energy is equal to the bolide kinetic energy) and dry sand scaling.

References: [1] Nemtchinov I. et al. (1997) *Icarus 130*, 259-274. [2] Brown P. et al. (2002) *Nature 420*, 294-296. [3] Shoemaker E. et al. (1970) *Science 167*, 452. [4] Moore J. et al. (1980) *Moon and Planets 23*, 231-252. [5] Neukum G. et al. (2001) *Chronology and Evolution of Mars*. Kluwer Academic Press, 55-86.. [6] Drozd R. et al. (1974) *Geochimica et Cosmochimica Acta 38*, 1625-1642. [7] Arvidson R. et al. (1975) *Moon 13*, 259-276. [8] Stuart J. and Binzel R. (2004) *Icarus 170*, 295-311. [9] Holsapple K. and Schmidt R. (1979) *Proc. LPSC 10th*. Pergamon Press, N.Y., 2757-2777. [10] Schmidt R. (1987) LPSC 18, 878-879. [11] Housen K and Holsapple K. (2003) *Icarus 163*, 102-119. [12] König B. et al. (1977) *LPSC 8th*, 555-556. [13] Hartmann W. (2005) *Icarus 174*: 294-32.